J Fluoresc (2014) 24:683–687
DOI 10.1007/s10895-014-1375-2

SHORT COMMUNICATION

Role of Rare Earth Oxide Nanoparticles (CeO_2 and La_2O_3) in Suppressing the Photobleaching of Fluorescent Organic Dyes

Anubhav Guha · Anindita Basu

Received: 15 November 2013 / Accepted: 19 March 2014 / Published online: 6 April 2014

Abstract Aqueous solutions with Rhodamine dye, and fluorescently labeled polymer samples of fibrin and collagen were mixed with aqueous dispersions of cerium oxide, lanthanum oxide, iron (II) oxide nanoparticles, and OxyFluor, a commonly used reagent for suppressing photobleaching. From time dependent studies of the fluorescence from these samples, we observed that the dyes in samples containing rare earth oxide nanoparticles exhibited significantly slower rates of fluorescence decay compared to control samples without additives, or containing OxyFluor or iron oxide nanoparticles. We posit that this may be related to the oxygen free radical scavenging properties of rare earth oxides.

Keywords Soft condensed matter · Dye fluorescence · Nanoparticles

Introduction

Photobleaching, or light-induced degradation of dyes, limits the lifetime of dyes by reducing their fluorescence over time. Suppressing this is important, for instance, in experiments related to the tagging of biomolecules with dyes, or in micro-rheological experiments on polymers that are treated with dyes in order to observe their flow characteristics over time, i.e., where it is important that the tagging dye last as long as needed for the observation [1]. Commercially, the effects of photobleaching on dyes can have detrimental effects on the longevity and visual appearance of products in the textile, paint, signage and display industries [2]. Thus, efficient and cheap reagents that slow the rate of photobleaching in dyes can have both scientific and industrial impact.

While the process of photobleaching is not fully understood, increased rates of photobleaching have been correlated with increased oxygen concentrations [3]. It is believed that an excited dye molecule can relax back to the ground state by exciting a ground state oxygen molecule into a reactive singlet state, which may, in turn, react with and quench the dye molecule [4, 5].

Oxides of rare earth (RE) and rare earth like metals such as cerium, lanthanum and yttrium are known possess ~~a~~ strong affinity for oxygen [6–10] and contain oxygen vacancy defects which allow them to scavenge oxygen from their surroundings. We hypothesize that RE oxide nanoparticles (NPs) may act as efficient scavengers of reactive oxygen species when added to fluorescent dye solutions, reducing the photobleaching of dyes. In this work, we show that small amounts of RE oxide nanoparticle additives such as CeO_2 and La_2O_3 indeed deter the photobleaching of dyes, thereby extending dye lifetimes. The effect is observed both for the cases of aqueous dye-nanoparticle dispersions, as well as in fluorescently labeled bio-polymer gels (collagen and fibrin) with small amounts of RE oxide nanoparticles added in. We find that these nanoparticles are more effective in suppressing photobleaching than a commercial alternative, OxyFluor™. In order to confirm the role of oxygen-deficient RE oxides on photobleaching, we compared the rate of photobleaching of dyes treated with FeO, an oxygen *excess*/iron deficient oxide, with the rates of photobleaching of dyes treated with CeO_2 and La_2O_3, both of which are oxygen *deficient* oxides. The results are consistent with the ability of the RE oxide

A. Guha
Horace Greeley High School, Chappaqua, NY 10514, USA

A. Basu (✉)
Department of Physics and Astronomy, University of Pennsylvania, Philadelphia, PA 19104, USA
e-mail: abasu@broadinstitute.org

Present Address:
A. Basu
School of Engineering and Applied Sciences, Harvard University, Cambridge, MA 02138, USA

nanoparticles to scavenge reactive oxygen species generated by the dye irradiation process.

Experiments

Three experiments were carried out. In Experiment 1, we studied the effect of addition of small amounts of La_2O_3 nanoparticles (diameters of 10–30 nm, 99.97 % purity) purchased from Sigma-Aldrich, USA, on the photobleaching properties of a solution of Rhodamine 6G dye in deionized distilled water (22.5 μg/ml). La_2O_3 is an oxygen deficient oxide, which allows the nanoparticles to absorb ambient oxygen molecules. Micro-capillary tubes were used to draw small volumes (0.44 mL) of three samples: (i) Rhodamine 6G solution only, (ii) Rhodamine 6G solution dispersed with La_2O_3 nanoparticles, and (iii) La_2O_3 nanoparticle dispersion only. The La_2O_3 nanoparticle dispersion was prepared by sonicating 25 mg La_2O_3 nanoparticles, 4 g ethylene glycol, and 250 mg sodium dodecylbenzenesulfonate (NaDDBS) in 20 g deionized distilled water for 4–6 h in a bath sonicator at 55 kHz. This dispersion was mixed with the Rhodamine solution at a volume ratio of 1:10 leading to a NP concentration of ~0.0065 wt%. The samples were then exposed to a focused 5 milliwatt laser (emission wavelength of 405 nm, fluence of ~0.64 W/cm^2) and the fluorescence spectra were measured every 30 s for 15 min using a JAZ spectrometer, Ocean Optics, USA.

In Experiments 2 and 3, we studied the ability of RE oxides with oxygen deficient stoichiometry like CeO_2 and La_2O_3 to reduce photobleaching in fluorescently labeled fibrin and collagen gels. Imaging studies of such biological polymeric materials are often carried out by labeling the biomaterials with fluorescent dyes. Commercial anti-photobleaching agent such as OxyFluor™, is often used to suppress photobleaching—however its action as an anti-photobleaching agent is short-lived, and is easily degraded by elevated temperature, vigorous handling, etc. Thus a hardier anti-photobleaching agent that allows for greater viewing periods for dyes is desirable.

Experiment 2 investigated the effect of CeO_2, which, like La_2O_3, is a RE oxide with an oxygen-deficient stoichiometry and oxygen vacancies in the crystal structure. Three samples of 200 μl of fluorescently labeled fibrin gels were prepared in T7 buffer solution (50 mM Tris, 150 mM NaCl at pH 7.4) at 1.5 mg/ml polymer concentration. Commercially available human fibrinogen, pre-conjugated with Alexa-Fluor 488 nm dye was purchased from Invitrogen, USA for this purpose. The CeO_2 dispersion was prepared at the same concentration and in the same manner as the La_2O_3 nanoparticles in Experiment 1. The first sample was prepared by adding 2 μl CeO_2 solution to the fibrin-dye mixture leading to a NP concentration of ~0.001 wt%. A second sample was prepared by adding 2 μl OxyFluor™, while a third sample, prepared without any anti-photobleaching agent, was used as a control.

The fibrin gels were then sealed between glass coverslips and exposed to a 488 nm wavelength laser, using a VTeye laser scanning confocal microscope (Visitech, UK), with 10 milliwatts of incident power distributed over a 75 μm×75 μm area (fluence~178 W/cm^2). The sample fluorescence was imaged every 30 s, for 120 s (resulting in 5 images per exposure area), in order to document the decay in fluorescence intensity with time. Four sets of images from four different locations on each polymer sample were obtained, to check for repeatability. The image intensities were then analyzed using ImageJ software, available from the National Institute of Health, USA. Fluorescent light intensities of randomly sampled image pixels were measured on a scale of 0–255 arbitrary units (henceforth referred to as a.u.) using ImageJ.

When the dyes are mixed with the polymeric gels, the dye molecules preferentially attach to the polymer protofibrils, resulting in regions where the dyes are aggregated at different concentrations, proportional to the local polymer concentration. Therefore when the fluorescence is imaged under a microscope the polymer/dye aggregations appear as distinct pockets of varying intensity. In this experiment it is therefore impossible to quantitatively measure local concentrations in these segregated pockets. Therefore, for each image set, the fluorescence decay was tracked as a function of time at three different points on the image with three different starting fluorescence intensities—250, 150, and 100 a.u. These represented three different local dye concentrations, viz., high, medium and low. The data was then averaged over the 4 image sets corresponding to the different regions of the same sample. These measurements were carried out for each of the three samples (i.e., samples with CeO_2, with OxyFluor, and the control sample "sans additives").

Experiment 3 was aimed at comparing the ability of oxygen deficient RE oxides (e.g., CeO_2, La_2O_3) versus an oxide known to have an oxygen excess stoichiometry, FeO [11], in diminishing photobleaching rates. If our hypothesis of oxygen scavenging is correct then one would expect the oxygen excess FeO to be less effective in reducing photobleaching rates. We prepared FeO nanoparticle suspensions in the same manner as the preparation for La_2O_3 described in Experiment 1. However, the solutions were mixed with a different dye (Rhodamine B, Sigma Aldrich, USA) and a different polymer gel, viz., 1.5 mg/ml collagen gel (Type I rat-tail collagen, BD Biosciences, USA) in 1× phosphate buffered saline at pH 7.4, in this experiment. This allowed us to check the efficacy of RE nano-particles in suppressing photo-bleaching for yet another dye with different excitation/emission spectra in a different biopolymer system. The results were recorded and analyzed in the same manner as Experiment 1, using ImageJ.

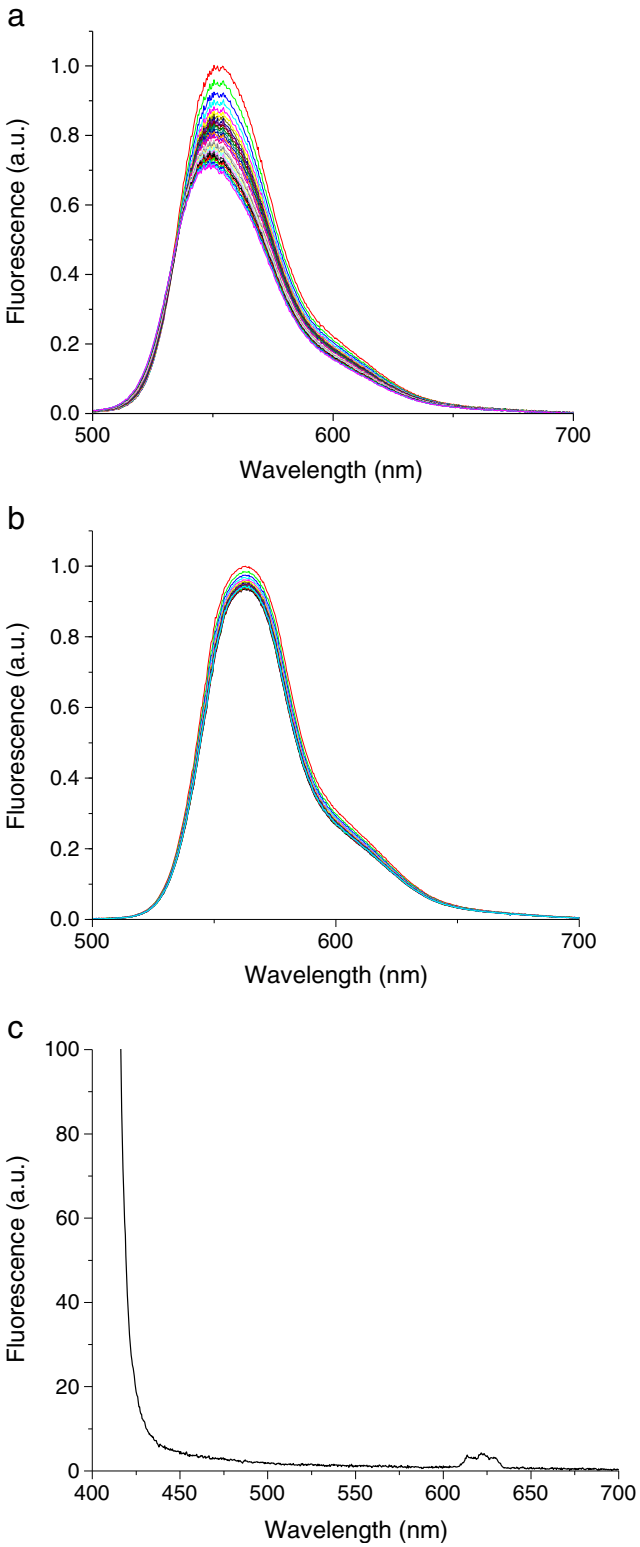

Fig. 1 Fluorescence intensity measured as function of wavelength for **a** Rhodamine sans additive solution; and **b** Rhodamine with La_2O_3 nanoparticle (NP) solution. The fluorescence intensity peak of the initial spectrum (taken at t=30 s) is normalized to 1 arbitrary unit (*a.u.*). Each subsequent plot is taken 30 s after the previous one. Figure 1(c) shows the fluorescence spectrum from the La_2O_3 NP solution in absence of the dye

Results and Discussion

The results of Experiment 1 are shown in Figs. 1 and 2. Figure 1a and b show fluorescence spectra from the dye without and with La_2O_3 NP additive, respectively, taken at 30 s intervals, under the same excitation conditions. Peaks centered around ~555 nm (dye solution without nanoparticles) and ~560 nm (dye solution with nanoparticles) are observed. The small shift in the peak could be due to changes in solvent polarity [12] or nanoparticle-dye interactions. We confirmed that the La_2O_3 solution itself did not fluoresce (Fig. 1c). The fluorescence counts were integrated from 450 to 800 nm from the spectra in Fig. 1a and b using standard routines available in Origin 8.6 software (OriginLab, USA) and the integrated fluorescence values are shown in Fig. 2 as a function of time. The incident laser power was observed to fluctuate by around 10 %, so error bars of ±5 % were included in the resultant graphs. It is clear from the figures that the dye solution with La_2O_3 NPs has a significantly reduced rate of photobleaching. The decreased rate of photodegradation of dyes in solution with La_2O_3 NP addition was reproducibly observed and also verified using a 500 nm excitation source in addition to the 410 nm excitation used in Experiment 1.

We see similar suppression in photobleaching in biopolymer gels labeled with Alexa Fluor 488 with the addition of RE oxide nanoparticles. Figure 3 shows the results for Experiment 2, where fluorescently labeled fibrin gels are tested for photobleaching with (i) CeO2, (ii) OxyFluor, (iii) 'sans additive' control, using a confocal microscope. It is clear that the

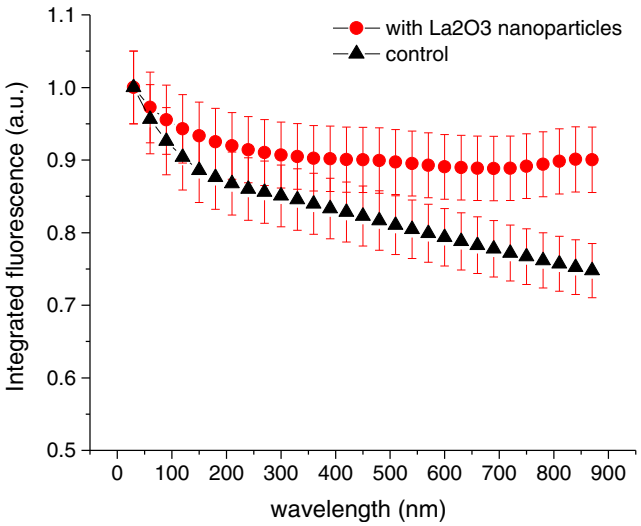

Fig. 2 Fluorescence intensities measured every 30 s and integrated between 400 and 800 nm are plotted for Rhodamine only solution (*black*), and Rhodamine and La_2O_3 NP solution (*red*). Integrated intensities are normalized to the integrated intensity at t=30s for both samples, given a value of 1 arbitrary unit. Total fluorescence values are calculated from fluorescence data shown in Fig. 1. Error bars of ±5 % arbitrary units of integrated fluorescence were assigned to the data points

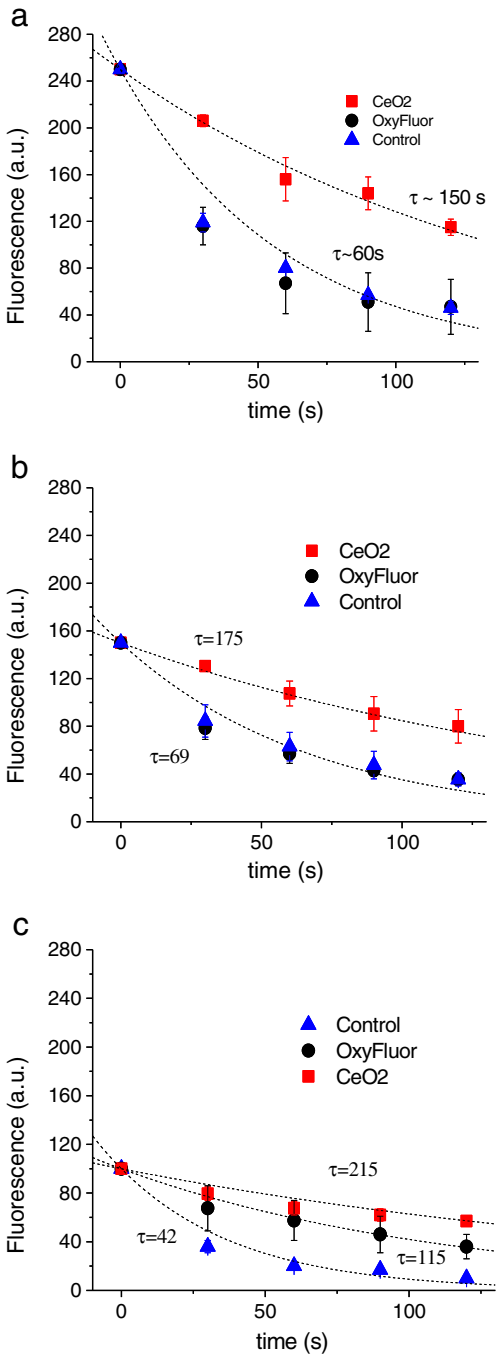

Fig. 3 Fluorescence intensities of AlexaFluor 488 labeled fibrin gels containing CeO_2 nanoparticles, OxyFluor, and control (sans additives) are plotted as functions of time. Initial emission intensities of **a** 250± 7 a.u., **b** 150±4 a.u., and **c** 100±4 a.u. represent regions of high, medium and low dye. The fluorescence intensity data are fitted (indicated by *dashed lines*) to an exponentially decaying function, $I=I_0 \exp(-\tau/t)$, where I_0 is the initial fluorescence intensity, I is the fluorescence intensity at any given time, t, and τ is the time constant of decay. Error bars represent the spread in the data that was used for averaging

CeO_2 nanoparticles are successful in suppressing photobleaching, and are more effective than the commercially available anti-photobleaching agent, OxyFluor, as well as the '*sans* additive' control, in all three cases of high (Fig. 3a), medium (Fig. 3b), and low (Fig. 3c) dye concentrations. The excitation conditions were identical for all of the cases, and the fluorescence intensities for the different cases are directly comparable to one another. Assuming that the rate of dye photobleaching at any given time, t, is proportional to the fluorescence intensity, I, at that time, we can fit the fluorescence data to an equation of exponential decay, viz., $I=I_0 \exp(-\tau/t)$ where τ is the time constant, and I_0 is the initial fluorescence intensity measured at $t=0$. The samples that are without additive have τ that varies from 42 to 69 s, while τ varies between 150 and 215 s for the samples with CeO_2 NP—an improvement of a factor of approximately 2.5 to 4—in suppressing photobleaching.

The results from Experiment 3, where we test fluorescently labeled collagen gels (Rhodamine B was used) for photobleaching using confocal microscopy, are shown in Fig. 4. The figure shows a clear difference between the samples containing RE oxides and the sample containing FeO. We observe that La_2O_3 and CeO_2 nanoparticles are similar in their ability to suppress photobleaching (τ~500 s) and perform significantly better than the FeO nanoparticles (τ~65 s). As mentioned earlier, FeO contains iron vacancy defects in its crystal structure that result in an oxygen excess stoichiometry, while CeO_2 and La_2O_3 contain oxygen vacancy defects in their crystal structure which allows them to absorb, transport and exchange oxygen with its environment [10]. The superiority of the rare earth oxides in suppressing photobleaching compared to FeO supports our hypothesis and is consistent with the expected mechanism of scavenging reactive oxygen species via RE oxide nanoparticles. We also note the solvent used to suspend NP (mix of water, ethylene glycol, and

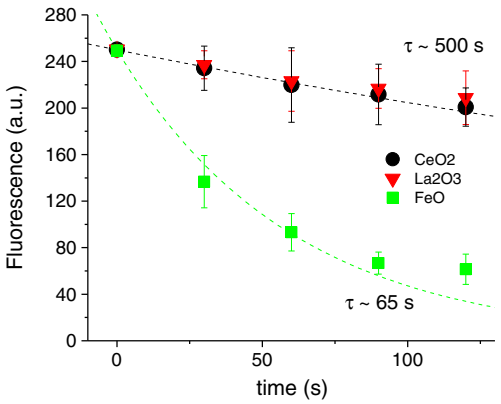

Fig. 4 Fluorescent intensities from collagen gel samples labeled with Rhodamine B and containing either La_2O_3, CeO_2, or FeO NP are plotted against time. Starting points have emission intensities of 250±4 a.u. Intensities between the different samples can be directly compared. The data are fitted to the exponentially decaying function described in Fig. 3. The time constant of decay, τ for the samples containing CeO_2 and La_2O_3 are ~500 s, and for the sample containing FeO is ~65 s. Error bars, calculated using the range of the data used to calculate the values of the points, are assigned to the points

NaDDBS) by itself did not prevent photobleaching. Though we did not conduct such an experiment directly, we witnessed this effect indirectly. When conducting experiments with the NP solutions that had not been sonicated for long enough, meaning that the NP were aggregated in large clusters, there was no suppression in photobleaching. Since the anti-photobleaching effect arises from the large surface area needed for oxygen absorption that is afforded in NP systems, it is crucial that the NPs are suspended well before each use. This may be done by resonicating the NP solution for 4 h at 55 kHz.

It is important to note that Experiment 3 should not be compared quantitatively to Experiment 2 since the polymer gels (collagen as opposed to fibrin), the dyes (Rhodamine B, fluorescing at 625 nm, as opposed to AlexaFluor 488 fluorescing at 519 nm) and the exciting laser wavelengths (568 nm as opposed to 488 nm), are not the same. The different systems were used to show the generality of RE nanoparticles as efficient anti-photobleaching agents for a variety of fluorescent dyes with different excitation/emission characteristics in different biopolymer systems.

From the concentrations of the RE nanoparticles used, we estimate that the average spacing of the nanoparticles was ~4–5 μm. The net result of this is that a large volume of dye can be protected from rapid photobleaching by a very small amount of the RE oxide nanoparticles, resulting in a cheap and effective solution to the photobleaching problem.

Conclusion

In summary, we found that very small amounts of nanoparticles of rare earth oxides such as CeO_2 or La_2O_3 with *oxygen deficient* stoichiometry were highly effective in suppressing the photobleaching of fluorescent dyes in both aqueous solutions as well as polymeric gels. The anti-photobleaching capabilities of the RE oxide NPs are superior to current commercially available alternative. Based upon our experiments with FeO NP which has an oxygen *excess* stoichiometry, we propose a model where rare earth oxide nanoparticles prevent the photobleaching of dyes due to their oxygen scavenging capability.

The addition of RE nanoparticles to dyes solutions in experiments where dyes are used as fluorescent markers would therefore prolong dye lifetimes and lend researchers a greater observation time. We note, however that for experiments in micro-rheology or biology, the morphology of the matrix may be altered by the addition of the RE oxide nanoparticles. For instance, bio-polymer gels are highly sensitive to pH, presence of cations, etc. [13]. We propose future work to investigate this effect, and exploring buffer solutions that can alleviate it. On the other hand it may be expected that the use of such nanoparticles may be useful in other applications, such as prolonging the lifetime of displays and signage under photo-exposure or moisture.

Acknowledgments We would like to thank Professor Arjun G. Yodh in the department of Physics and Astronomy, and Director of the Laboratory for Research on the Structure of Matter at the University of Pennsylvania for the opportunity of performing the experiments in his lab, and helpful suggestions. We would also like to thank Mr. Ted van Kessel and Dr. Siyuan Lu (both at IBM T.J. Watson Research Center) for useful discussions and suggestions.

References

1. Pinaud F, Dahan M (2011) Targeting and imaging single biomolecules in living cells by complementation-activated light microscopy with split-fluorescent proteins. Proc Natl Acad Sci 108:201–210
2. Macdonald AM, Wyeth P (2006) On the use of photobleaching to reduce fluorescence background in raman spectroscopy to improve the reliability of pigment identification on painted textiles. J Raman Spectrosc 37:830–835
3. Hartmann P, Leiner M, Kohlbacher P (1998) Photobleaching of a ruthenium complex in polymers used for oxygen optodes and its inhibition by singlet oxygen quenchers. Sensors Actuators B 51:196–202
4. Chen TS, Zeng SQ, Zhou W, Luo QM (2003) A quantitative theory model of a photobleaching mechanism. Chin Phys Lett 20:1940–1943
5. Song L, Hennink EJ, Young IT, Tanke H (1995) Photobleaching kinetics of fluorescein in quantitative fluorescence microscopy. Biophys J 68:2588–2600
6. Schubert D, Dargusch R, Raitano J, Chan SW (2006) Cerium and yttrium oxide nanoparticles are neuroprotective. Biochem Biophys Res Commun 342:86–91
7. Ka X, Robertson J (2009) Oxygen vacancies in high dielectric constant oxides La_2O_3, Lu_2O_3, and $LaLuO_3$. Appl Phys Lett 95: 22903–22903-3
8. Babu S, Velez A, Wozniak K, Szydlowska J, Seal S (2007) Electron paramagnetic study on radical scavenging properties of ceria nanoparticles. Chem Phys Lett 442:405–408
9. Tarnuzzer R, Colon J, Patil S, Seal S (2005) Vacancy engineered ceria nanostructures for protection from radiation-induced cellular damage. Nano Lett 5:2573–2577
10. Kalenik Z, Wolf EE (1992) Transient isotopic studies of the role of lattice oxygen during oxidative coupling of methane on sr promoted lanthanum oxide. Catal Today 13:255–264
11. Genioz R, Hazen RM (1983) Compression, nonstoichiometry and bulk viscosity of wustite. Nature 304:620–622
12. Zakerhamidi MS, Moghadam M, Ghanadzadeh A, Hosseini S (2012) Anisotropic and isotropic solvent effects on the dipole moment and photophysical properties of rhodamine dyes. J Lumin 132:931–937
13. Jiang F, Hörber H, Howard J, Müller DJ (2004) Assembly of collagen into microribbons: effects of pH and electrolytes. J Struct Biol 148: 268–278